Color Digital Halftoning Taking Colorimetric Color Reproduction Into Account

Hideaki Haneishi, Toshiaki Suzuki, Nobukatsu Shimoyama, and Yoichi Miyake
Chiba University Department of Information and Computer Sciences
1-33 Yayoi-cho, Inage-ku, Chiba 263, Japan
E-mail: haneishi @ics.tj.chiba-u.ac.jp

Abstract

Taking colorimetric color reproduction into account, the conventional error diffusion method is modified for color digital halftoning. Assuming that the input to a bilevel color printer is given in CIE-XYZ tristimulus values or CIE-LAB values instead of the more conventional RGB or YMC values, two modified versions based on vector operation in (1) the XYZ color space and (2) the LAB color space were tested. Experimental results show that the modified methods, especially the method using the LAB color space, resulted in better color reproduction performance than the conventional methods. Spatial artifacts that appear in the modified methods are presented and analyzed. It is also shown that the modified method (2) with a thresholding technique achieves a good spatial image quality.

1 Introduction

Many digital halftoning techniques including fixed pattern, ordered dither, and error diffusion have been developed to produce an illusion of a continuous tone image with a bi-level printer.[1–4] As color bilevel printers, such as ink jet printers, have become more widely used, color digital halftoning methods have been developed along with monochromatic digital halftoning.[5,6] The need for higher image quality and the increasing performance of digital hardware such as DSP indicates that error diffusion (ED) among many possible algorithms may be the most promising as a fundamental algorithm.

When color digital halftoning is used in an image transmission application such as a color facsimile, reproduction of the original color at the receiving site becomes very important. This issue is addressed as device independent color reproduction. To achieve colorimetric color reproduction between different display devices in color image transmission, it is necessary to use a common color space such as CIE tristimulus values, XYZ, or CIE uniform color space, LAB, rather than the device dependent RGB or YMC representation. In the near future, we believe such color spaces will be adopted as the standard parameters describing color.[7,8] For the devices that produce continuous tone, many color matching techniques have already been developed.[9,10] However, for color digital halftoning, there have been only a few approaches in establishing the use of a standard color space.[11–13]

The eight dotwise colors reproduced by a bilevel color printer with yellow, magenta, and cyan inks are as follows: white (W) of paper itself, yellow (Y), magenta (M), and cyan (C) as the first-order colors, and red (R), green (G), and blue (B) as the second-order colors, with black (K) as the third-order color. Here, we define these eight colors as the primary colors. When the primary colors are spatially distributed in a small area with a certain area ratio, a mixed color of these primary colors is perceived by the human visual system. According to Neugebauer, a simple model that estimates such a color mixture is given by linear combinations of tristimulus values of the primary colors with the corresponding area ratio.[14,15]

In the simplest color ED method using, Y, M, C separations, each component of the color image is individually processed just as the monochromatic version, resulting in a calculated dot pattern. In the actual case, first the original Y, M, C separations are color corrected through a masking operation and then the ED algorithm is applied to generate a dot pattern. Even in such a case, however, the dot pattern generated by superposition of three individually processed components is not controlled systematically and therefore colorimetric color reproduction is not guaranteed inherently.

In this paper, we extend the ED algorithm to the color vector space. When an input image to be processed is given in vector form composed of XYZ or LAB values and the XYZ or LAB values of the eight primary colors used are also known, the proposed method can generate a proper dot pattern in a one-step systematic way based on vector operation, which can potentially produce a colorimetrically correct image. Two ED methods using the color vector spaces, XYZ and LAB, are tried here. This paper explores not only the proposal of vector operations using the standard color space, but also the comparison of the color spaces used and the introduction of a technique to remove a smear artifact that appears in the vector ED method.

2 Methods

2.1 Scalar Method

First, we review the ED algorithm for a monochromatic image. If the original or objective pixel value f_{mn} at the location (m,n) is expressed in 8 bits, the range of value is

$$0 \le f_{mn} \le 255. \tag{1}$$

For each pixel, the final bilevel value v_{mn} is given by the following equations,

$$v_{mn} = \begin{cases} 255, & \text{for} \quad x_{mn} > t \\ 0, & \text{for} \quad x_{mn} \le t \end{cases}, \tag{2}$$

$$x_{mn} = f_{mn} + \sum_{ij} w_{ij} e_{m+i,n+j}, \tag{3}$$

$$e_{m+i,n+j} = x_{m+i,n+j} - v_{m+i,n+j}. \tag{4}$$

Namely, the corrected value x_{mn} is given by a summation of the objective value f_{mn} and the weighted combination of the error $e_{m+i,n+j}$ caused by binarization at the neighboring pixels. The typical weights $\{w_{ij}\}$ originally used by Jarvis, Judice, and Ninke[2] are given in Fig. 1. The corrected value x_{mn} is compared with a predetermined threshold level t (usually 128) and the final level is determined according to Eq. (2). This process is repeated pixel by pixel in the raster scan fashion over the entire picture.

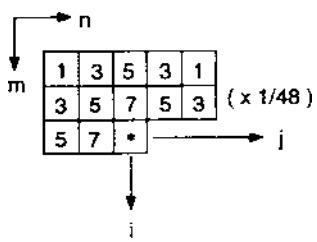

Figure 1. Weights $\{w_{ij}\}$ proposed by Jarvis, Judice, and Ninke[2] for the ED algorithm.

As mentioned in the previous section, in the simplest color digital halftoning where the above operation is carried out for each color component independently, the colorimetric color reproduction is not guaranteed. In this paper, this method is called a scalar method and is compared with the modified methods using vectors.

2.2 XYZ Method

We modified the above method in two ways. The underlying idea of the modified versions is similar to the monochromatic version. The differences lie in that color is treated by vector rather than scalar. The two vector ED methods are different with respect to the usage of color space. In the following explanation **f**, **e**, **x**, and **v** denote a vector whose elements are the X, Y, Z values and **f′**, **e′**, **x′**, and **v′** denote a vector whose elements are the L^*, a^*, b^* values. The components of a LAB vector are derived from those of the corresponding XYZ vector as

$$L^* = 116(Y/Y_n)^{1/3} - 16, \tag{5}$$

$$a^* = 500[(X/X_n)^{1/3} - (Y/Y_n)^{1/3}], \tag{6}$$

$$b^* = 200[(Y/Y_n)^{1/3} - (Z/Z_n)^{1/3}], \tag{7}$$

where X_n, Y_n, Z_n are the XYZ values for the reference white.[16]

In the first modified method, a corrected vector and an error vector are calculated in the XYZ color space as

$$\mathbf{x}_{mn} = \mathbf{f}_{mn} + \sum_{ij} w_{ij} \mathbf{e}_{m+i,n+j} \tag{8}$$

$$\mathbf{e}_{m+i,n+j} = \mathbf{x}_{m+i,n+j} - \mathbf{v}_{m+i,n+j}. \tag{9}$$

The weights are same as the scalar method; $\mathbf{f}_{mn}$ is an objective color and $\mathbf{v}_{m+i,n+j}$ is one of eight primary colors. The choice of a color from eight primary colors is done by the following equation:

$$\mathbf{v}_{mn} = \mathbf{v}_l \left| \min\{\|\mathbf{x}_{mn} - \mathbf{v}_l\|\}, \right. \tag{10}$$

where $\|\cdot\|$ denotes the Euclid norm of a vector. The above equation means that the primary color closest to the vector $\mathbf{x}_{mn}$ is chosen. For example, if red among the eight primary colors is closest to $\mathbf{x}_{mn}$, magenta and yellow become ON and cyan OFF at the location (m,n).

This way of using the XYZ color space is a straightforward approach in the sense that the perceived color for the mixture of color microdots is reasonably modeled in the XYZ color space as is the case with the Neugebauer equations.[14]

2.3 LAB Method

If the LAB color space is used as the standard color signal, the algorithm using a LAB vector instead of the XYZ vector is easier to implement. Namely, the corrected vector and the error vector are calculated in the LAB color space as

$$\mathbf{x}'_{mn} = \mathrm{f}'_{mn} + \sum_{ij} w_{ij} \mathbf{e}'_{m+i,n+j} \tag{11}$$

and

$$\mathbf{e}'_{m+i,n+j} = \mathbf{x}'_{m+i,n+j} - \mathbf{v}'_{m+i,n+j}. \tag{12}$$

The choice of color is also based on the Euclid norm in the LAB color space as

$$\mathbf{v}'_{mn} = \mathbf{v}'_l \left| \min\{\|\mathbf{x}'_{mn} - \mathbf{v}'_l\|\}. \right. \tag{13}$$

It should be noted that if linear combinations of XYZ values of primary colors used give a good approximation for perceived color for microdots, linear combinations of the LAB vector obtained by nonlinear transformation of XYZ might not be a good approximation, conversely.

2.4 Smear Reduction

As we will show in the next-section, when we use the vector ED methods, two kinds of unfavorable artifacts appear around some transition areas of color. We call these artifacts the slow response and smear in this paper. These artifacts do not appear in the case of the scalar ED method. Detailed analysis of these artifacts will be given in a later section. Here we briefly show a cause of the smear artifact and give a solution to the problem.

When a color gamut spanned by primary colors is distorted, vector ED algorithms tend to produce a large error vector **e** during an ED process for uniform color area although the resultant dot pattern is stable. After the process reaches the transition area, it spends many pixels to cancel the large residual error in the following color area. As a result, unfavorable color different from the objective color appears there.

A simple way to reduce such smear is to neglect large color differences in the transition area. Namely, if the difference between the objective color **f** and the corrected colors **x** of the neighboring pixels exceeds a predetermined threshold, this is regarded as a transition area, and the errors are omitted in the ED process. The detailed flow of this procedure is shown in Fig. 2.

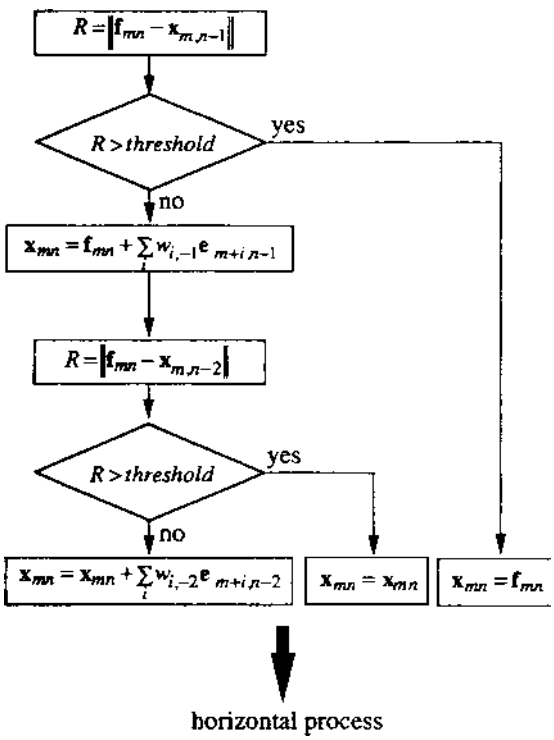

Figure 2. Procedure for smear reduction using threshold technique. Only the vertical process is presented. The horizontal process similar to the vertical process is carried out successively.

3 Experiment

To compare the performance of the scalar and two vector methods, we applied the above algorithms to several sample images and evaluated the resulting halftone images. The printer used in this experiment is a silver halide type printer (Fuji, Pictrography 3000). Although this printer can produce 24 bits full color (8 bits × 3 dyes), we used only the maximum (255) and minimum (0) level for each dye when we simulated a bilevel color printer.

In the proposed methods, it is necessary to know the XYZ values of eight primary colors. Thus, we first printed these solid color patches and measured the colors of each patch by a spectrophotometer (ICS-Texicon, SF-500). Table 1 shows the XYZ and LAB values of eight primary colors of the Fuji printer. In the calculation of the LAB values, we used XYZ values of the paper itself used in the printer as the reference white. Figure 3 gives the location of eight primary colors in each three-dimensional space. It should be noted for the later discussion that the color gamut spanned by eight primary colors in XYZ color space is very thin and distorted.

Table 1. XYZ and LAB values of eight primary colors.

Primary color	X	Y	Z	L*	a*	b*
White	76.8	80.4	92.4	100	0.0	0.0
Yellow	58.2	65.9	18.1	92.6	-11.9	71.0
Magenta	33.0	19.1	39.9	55.9	67.5	-27.2
Cyan	23.6	35.3	62.4	72.2	-42.6	-23.5
Red	17.1	9.4	1.2	40.7	58.6	51.3
Green	17.3	29.8	8.3	67.3	-54.9	54.1
Blue	5.1	4.9	21.2	29.7	4.8	-43.6
Black	0.6	0.7	0.7	7.8	-1.4	2.4

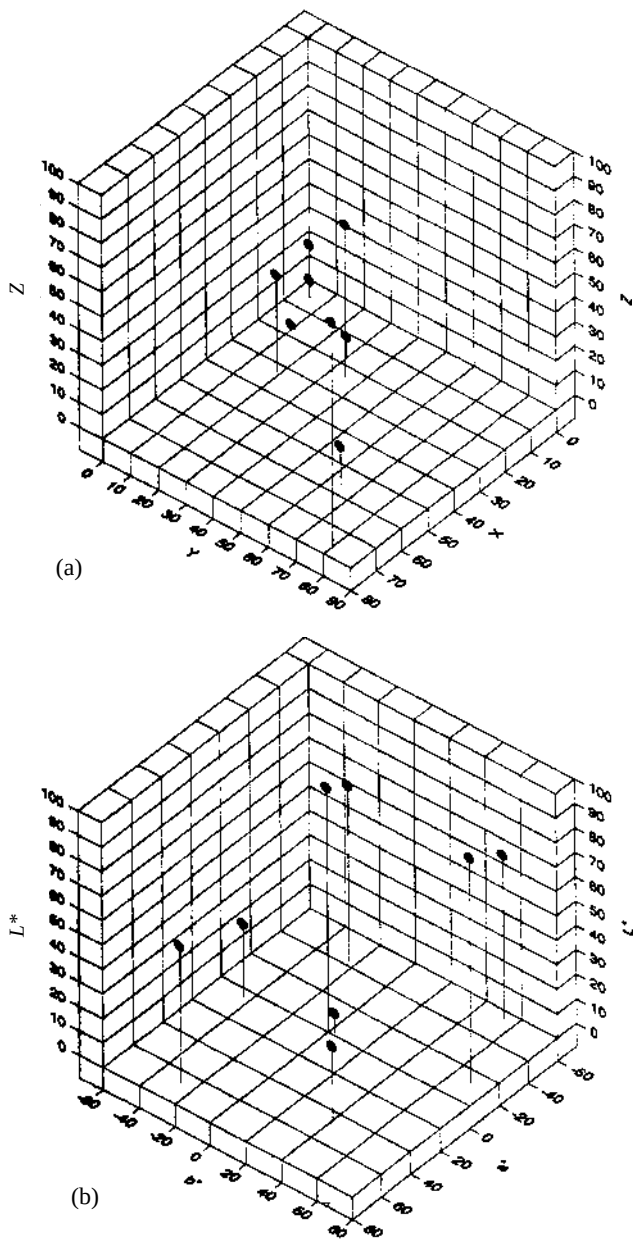

Figure 3. Location of eight primary colors of the printer used: (a) XYZ color space and (b) LAB color space.

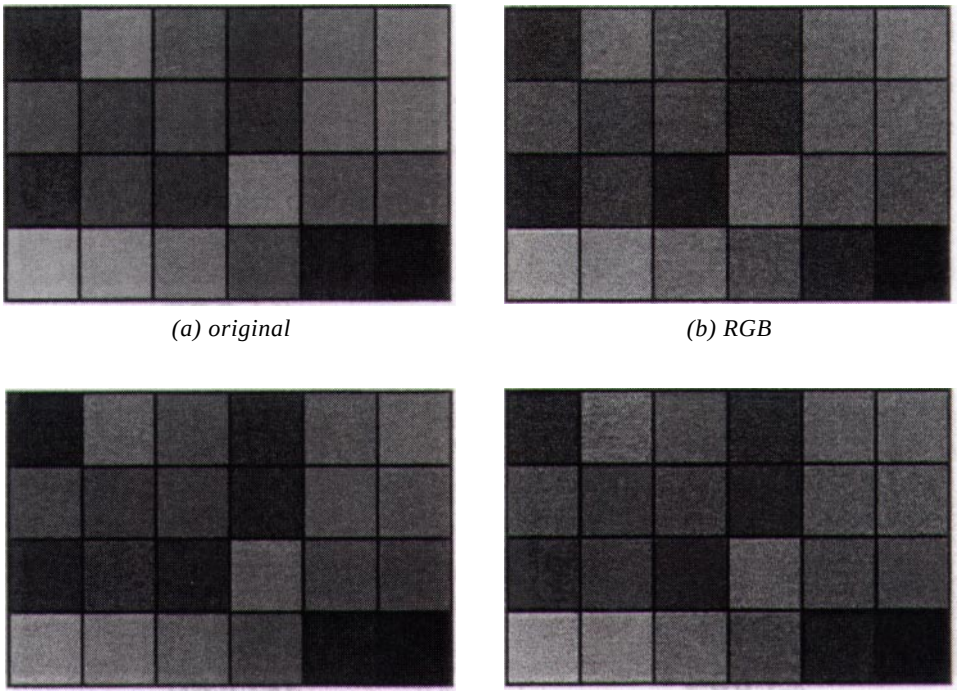

(a) original *(b) RGB*

(c) XYZ *(d) LAB*

Image #1

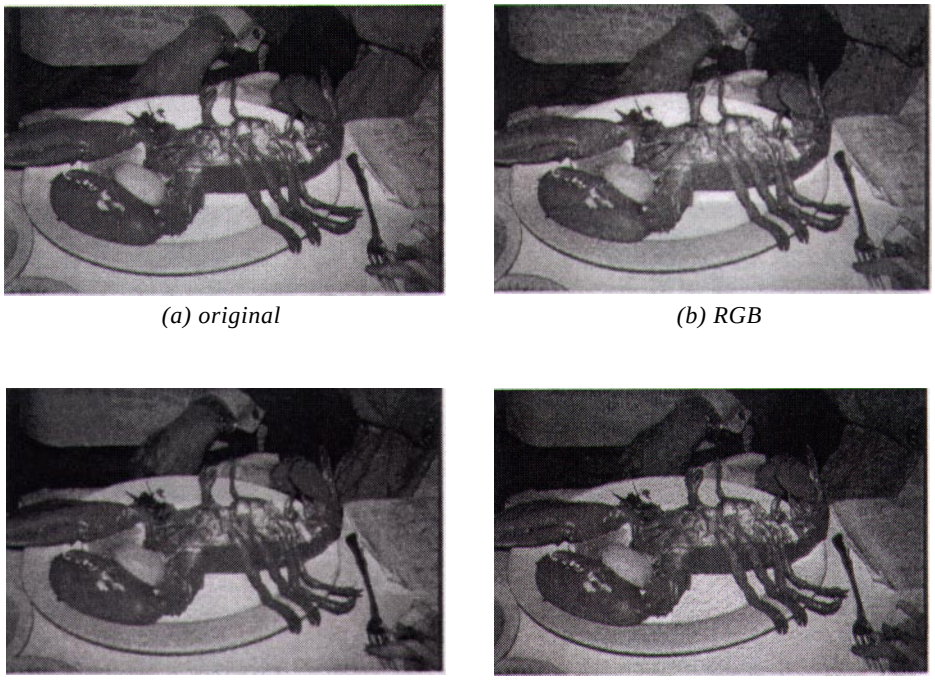

(a) original *(b) RGB*

(c) XYZ *(d) LAB*

Image #2

Figure 4. Original samples and halftone images: (a) the original (objective) images, (b) the scalar (RGB) method, (c) the XYZ method, and (d) the LAB method. *(Continued on next page.)*

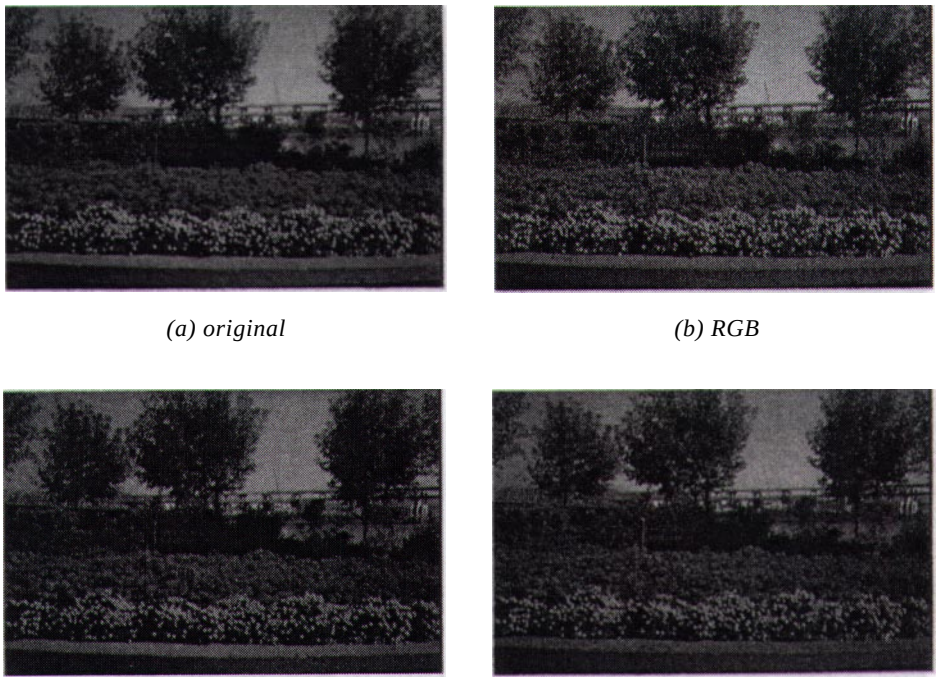

(a) original *(b) RGB*

(c) XYZ *(d) LAB*

Image #3

Figure 4. Continued

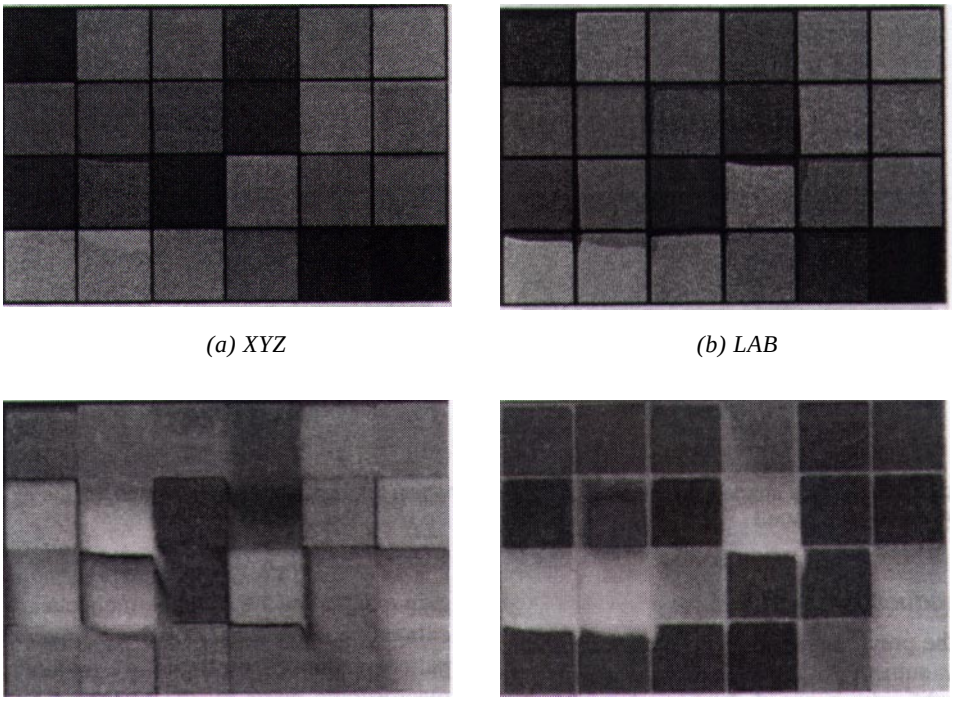

(a) XYZ *(b) LAB*

(c) XYZ *(d) LAB*

Figure 5. The halftone images of the Machbeth checker generated without smear reduction operation (a) and (b) and the error images (c) and (d).

The (a) images in Fig. 4 show three original samples used in the experiment. The image size is 760×512 pixels. Image number 1 is a Machbeth color checker, which is mainly used for quantitative evaluation with respect to color reproduction. Image numbers 2 and 3 are pictorial images, which were used for subjective evaluation with respect to color reproduction and spatial image quality.

Each sample image originated from digital R, G, and B values (8 bits $\times$ 3 channels). In the scalar ED method, these values were used as input data as they are. In the vector methods, objective images must be given by XYZ or LAB values. We regarded the sample images printed by the above-mentioned printer with full color as the objective images. The XYZ values of the printed images were estimated in the following way. First the relationship between input signal R, G, B and actually produced color X, Y, Z were calculated in advance using 125 color patches uniformly selected from the RGB space. Then we estimated XYZ values of a printed image, pixel by pixel, from the original RGB values by using the above relationship. The LAB values were calculated from the estimated XYZ values according to Eqs. (5) to (7).

Some error may exist in the estimation of XYZ values because of the small number of color patches used in the calibration. Though the estimated XYZ image would not have any problem in spatial quality evaluation and rough evaluation of color reproduction, it is not suitable for critical evaluation of color reproduction. Thus, an accurate quantitative evaluation was carried out with the Machbeth checker. We directly measured the color of 24 patches in the originally printed Machbeth checker by the spectrophotometer and regarded those values as the objective colors. The color patches in the halftone images generated by the ED methods were also measured similarly, and the color differences between the objective and resultant colors were calculated.

First we will show the spatial artifacts in the vector ED methods. Figures 5(a) and 5(b) show the halftone images of the Machbeth checker with the artifacts. The slow response artifact appears at e.g., (2, 1) (2nd row, 1st column), (2, 6) (3, 4) patches in Fig. 5(a). The smear artifact appears at (3, 2), (4, 2) in Fig. 5(a) and (3, 4), (4, 1), (4, 2), etc. in Fig. 5(b). These artifacts tend to expand down. The vector ED methods were applied to the pictorial images as well. As a result, any visible artifact did not appear when using the LAB color space, while both artifacts appeared and the resulting image quality was very poor when using the XYZ color space.

As far as the smear artifact is concerned, we can clearly show that the artifact highly relates to the accumulation of the error vector. Namely, Figs. 5(c) and 5(d) are the error images defined by $\|\mathbf{x}_{mn} - \mathbf{f}_{mn}\|^2$ in which the bright parts represent large error and their bottom areas correspond to the smear artifact in Figs. 5(a) and 5(b). It will be shown below that these artifacts are fairly reduced by the thresholding technique.

Figures 4(b) to 4(d) show the resultant images generated by the scalar and vector ED methods. In all results by the vector ED methods, the thresholding operation is adopted. The threshold level was set to be 50, which was decided empirically after some trials. This set of the level was rather robust. It took about 10 to 20 s to generate a halftone image using the vector ED methods by a micro SPARC II compatible workstation (Japan Computer Corp.)

First, we consider the spatial quality of the images. In the LAB method, the smear is successfully reduced and its spatial quality is fairly good as is the case of the scalar (RGB) method. In the XYZ method, though the smear artifact is reduced, the slow response is not improved. As a result, the spatial quality remains relatively poor.

Next, let us focus on the color reproduction performance. Using 24 color patches in the Machbeth checker, the color differences were evaluated in both the XYZ color space and the LAB color space by the equations defined as follows:

$$\Delta E_{XYZ} = \left[(X_{rep} - X_{obj})^2 + (Y_{rep} - Y_{obj})^2 + (Z_{rep} - Z_{obj})^2\right]^{1/2}, \tag{14}$$

$$\Delta E_{LAB} = \left[(L^*_{rep} - L^*_{obj})^2 + (a^*_{rep} - a^*_{obj})^2 + (b^*_{rep} - b^*_{obj})^2\right]^{1/2}, \tag{15}$$

where the subscripts *rep* and *obj* denote *reproduction* and *objective*, respectively. The former would be a suitable measure for the XYZ method based on the Neugebauer theory. For human visual system, however, the difference in the LAB color space should be a better measure and better correlate to subjective evaluation.

The average color differences over 24 colors are summarized in Table 2. The individual values of ΔE_{LAB} are also shown in Fig. 6. As we expected, the vector methods achieved better reproduction than the scalar method. The LAB method is superior to the XYZ method with respect to color reproduction as well as spatial quality. For the pictorial images, we still feel that the color reproduction of the vector methods is better than the RGB method, especially for reddish objects or blue sky.

Table 2. Average color differences (measured).

Color space	ΔE_{XYZ}	ΔE_{LAB}
RGB	5.4	12.5
XYZ	3.4	6.7
LAB	2.8	4.4

4 Discussion

In this section, we will discuss the difference between two presented vector ED methods in color reproduction and then analyze the slow response and smear problems through computer simulation.

4.1 Color Reproduction

As mentioned in the previous section, if the color reproduction were exactly subject to the Neugebauer theory, the XYZ method should achieve much better color reproduction. To confirm this expectation, we predicted the color reproduction under the ideal printing characteristics, where each microdot produces the solid

color exactly and no dot gain exists. For the Machbeth checker, we numerically calculated each area ratio of the primary colors from the dot pattern generated by the above methods, and predicted the macroscopic color by the weighted linear combination of the primary colors. Then we calculated the color difference from the objective colors. The result is shown in Table 3. As expected, the XYZ method provides the best color reproduction. The values are not zero even in the ideal model because the average is calculated over a finite area that usually has any error to be diffused to the outside of the area.

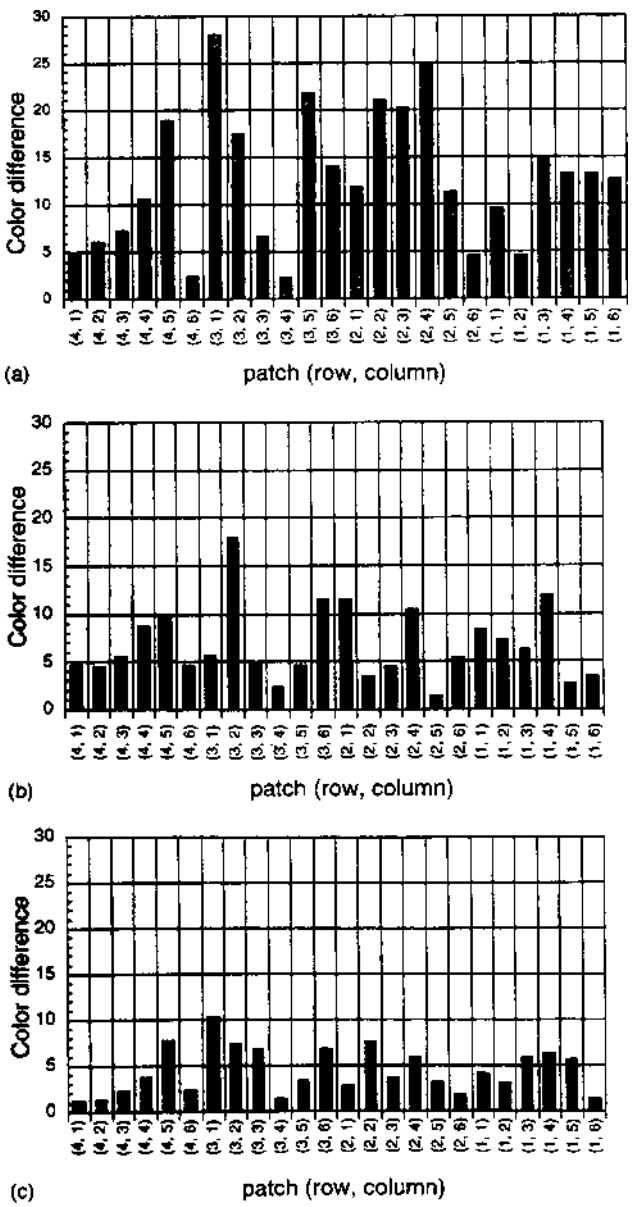

Figure 6. Color differences ΔE_{LAB} for each color patch: (a) the scalar method, (b) the XYZ method, and (c) the LAB method.

Table 3. Average color differences (calculated).

Color space	ΔE_{XYZ}	ΔE_{LAB}
RGB	13.6	18.5
XYZ	0.3	1.7
LAB	16.1	11.9

The fact that the color reproduction performance of the XYZ method is better than the LAB method is inconsistent with the experimental results and implies that in the actual printing system used, each microdot does not produce the ideal density profile. Thus, in future work we have to take the characteristics of the actual printing system into account and further modify the algorithm in order to achieve better color reproduction. After that, we need to compare the proposed methods again.

4.2 Analysis of Spatial Artifact

Through computer simulation, we analyzed causes and characteristics of the slow response and smear problems when the ED algorithm is applied in vector manner. To understand the problems simply and visually, we assume that only two inks, i.e., *Y* and *M*, are used, and consequently the halftone image is generated by four primary colors, *Y, M, W, R*. The dimension of color space was also reduced to two for simplicity. A spatially uniform color image with 256 × 256 pixel size was established as an objective image.

In the scalar method, the objective color was set to be $(Y_o, M_o) = (0.55, 0.54)$. *Y* and *M* were independently processed here and the resultant halftone image shown in Fig. 7(a) was obtained. The behavior of the ED process along with the central vertical line ($n = 128$) of the image was traced. In Fig. 8(a), four apexes of the square correspond to four primary colors and the symbol ❑ near the center of it gives the objective color. In this square, only the horizontal value is used for the *Y* separate image, while only the vertical value is used for the *M* separate image. Black dots in the figure give the corrected values along with the central vertical line, defined by

$$Y_{m,128} = Y_o + \sum w_{ij} e_{m+i,128+j},$$

$$M_{m,128} = M_o + \sum w_{ij} e_{m+i,128+j}.$$

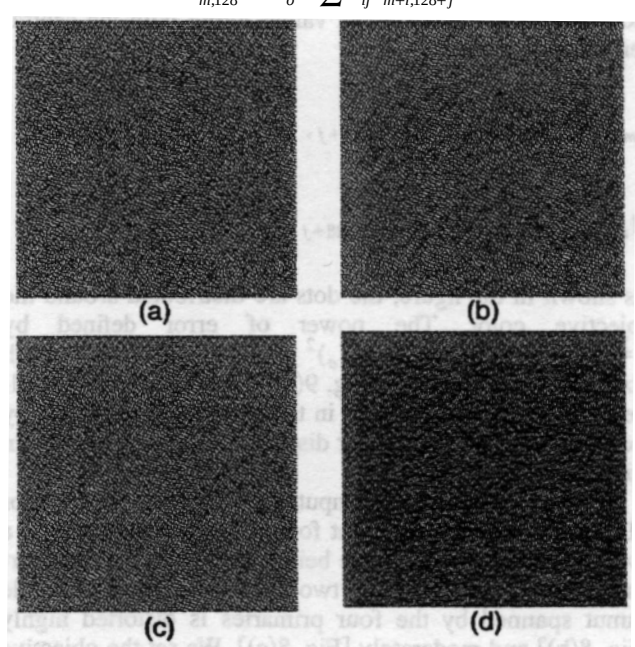

Figure 7. Halftone images generated by (a) the scalar method, (b) the vector method in the case of highly distorted color gamut, (c) the vector method in the case of moderately distorted color gamut, and (d) the vector method with Floyd fiber.

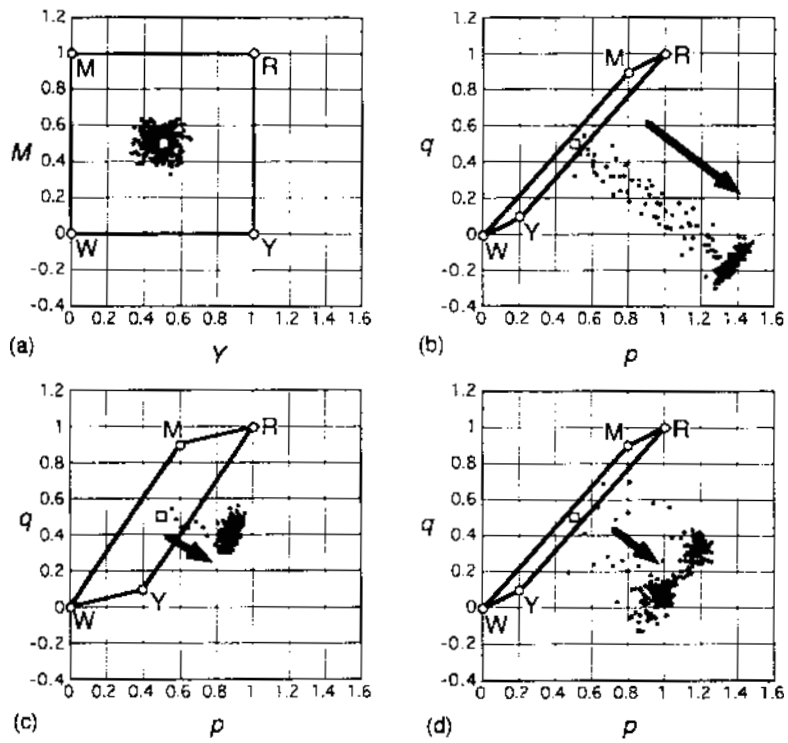

Figure 8. Corrected vector $\mathbf{x}_{mn}$ along with the central vertical line. Items (a) to (d) correspond to those of Fig. 7. The symbol ❑ represents the objective color.

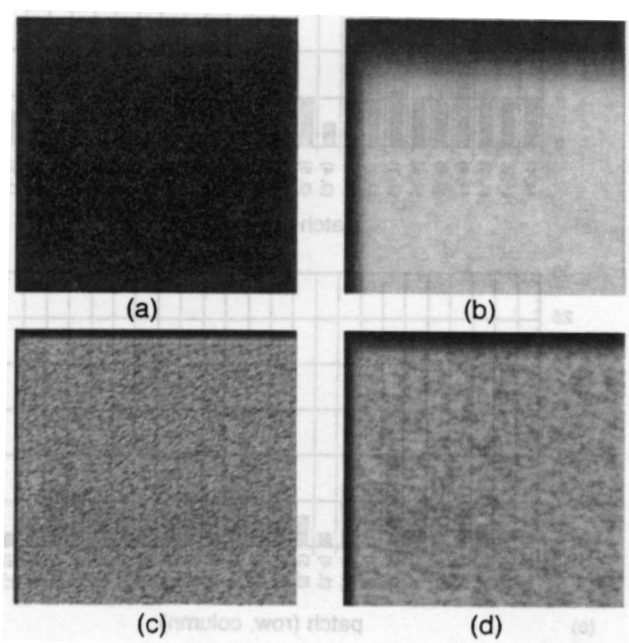

Figure. 9. Error images defined by the power of deference between the objective and corrected vector. Items (a) to (d) correspond to those of Fig. 7.

As shown in the figure, the dots are distributed around the objective color. The power of error defined by $E = (Y_{mn} - Y_o)^2 + (M_{mn} - M_o)^2$ was also calculated at each pixel, which is shown in Fig. 9(a). The values are normalized by the maximum value in the image and displayed by the bright level. Biased error distribution is not observed in this case.

Next, we present the computer simulation of the vector ED method. We assume that four primary colors are on a two-dimensional color plane being defined by the p,q coordinate. Let us consider the two cases where the rectangle gamut spanned by the four primaries is distorted highly [Fig. 8(b)] and moderately [Fig. 8(c)]. We set the objective color to be $\mathbf{f}_o = (p,q) = (0.55,0.54)$ and applied the vector ED to this objective image. The corrected vectors $\mathbf{x}_{m,128} = \mathbf{f}_o + \sum w_{ij}\mathbf{e}_{m+j,128+j}$ are plotted by black dots in Figs. 8(b) and 8(c). In the figures, the general trend of the corrected vector along with the central vertical line in the image. The power of the error vector defined by $\|\mathbf{x}_{mn} - \mathbf{f}_{mn}\|^2$ is visualized as shown in Figs. 9(b) and 9(c).

In the case of vector ED, it is found that the corrected vector $\mathbf{x}_{mn}$ is distributed away from the objective color $\mathbf{f}$. Especially for the highly distorted gamut, the converged area of $\mathbf{x}_{mn}$ is very far from $\mathbf{f}_o$ and it takes a long time to reach there. Since in the upper or starting area of the image, the primary colors Y and M are close to the corrected color $\mathbf{x}_{mn}$, only those colors are used to generate a halftone. The third color R participates in the halftone generation later. This varying dot pattern along the vertical direction can be observed in the resultant halftone image in Fig. 7(b). This slow artifact is similar to the (2,1) or (2,6) patch in Machbeth pattern of Fig. 5(a). Considering the extension of this behavior to the actual case with three dimensions, we could say that the nonuniform distribution of primary colors causes the slow response. The fact that the LAB method has faster

response than the XYZ method may result from the distribution of primary colors being more uniform, as shown in Fig. 3.

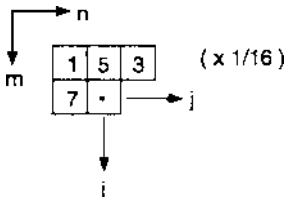

Figure 10. Weights $\{w_{ij}\}$ proposed by Floyd et al. for the ED algorithm.

When the objective image is the Machbeth checker, the residual error vectors at the end of the patch are transferred to the next patch. These vectors, however, may be fairly large in cases such as Fig. 8(b). The following patch has to spend many pixels to cancel this error. It leads to the smear artifact, as typically appeared in Figs. 5(a) and 5(b). Since the proposed thresholding process omits the large error vectors at the boundary of the color patches, the smear artifact can be reduced.

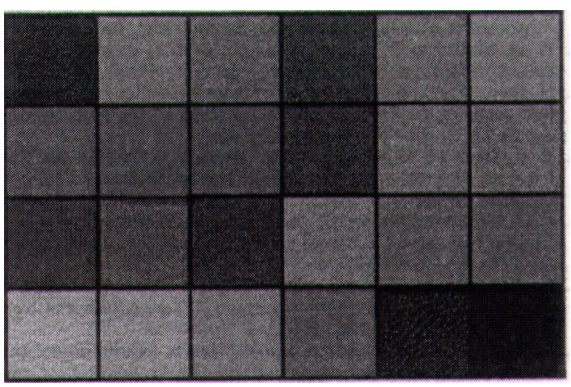

(a) XYZ

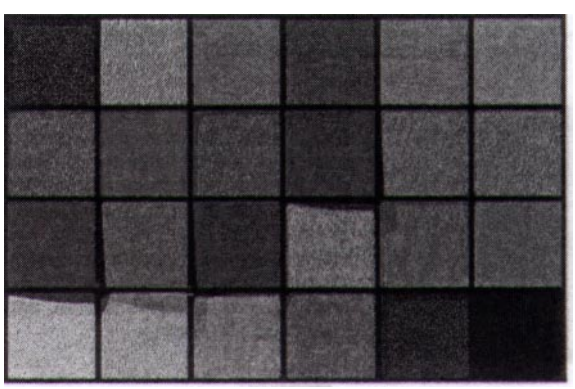

(b) LAB

Figure 11. Halftone images of the Machbeth checker generated with Floyd filter: (a) XYZ method and (b) LAB method.

We have also investigated the effect of the filter size through simulation. A smaller filter proposed by Floyd and Steinberg shown in Fig. 10 was applied to the highly distorted case. The resultant halftone image, corrected vector, and error image are shown in Figs. 7(d), 8(d), and 9(d), respectively. Compared to the case of the Jarvis filter, the dot pattern became stable faster. The Floyd filter was then applied to the Machbeth checker. Figure 11 shows the resultant halftone images. Though the slow response in the XYZ case was improved, unfavorable texture appeared in some patches. Judging from all the experimental results obtained, it is suggested that the vector ED algorithm with the Jarvis filter in the LAB color space achieves the most excellent image quality.

5 Conclusions

Taking colorimetric color reproduction into account, we modified conventional or scalar ED for color digital halftoning. Assuming that the input to a bilevel color printer is given in XYZ or LAB values instead of RGB or YMC values, we tested two vector ED methods, one using the XYZ color space and the other using the LAB color space. We also analyzed the spatial artifacts appearing in the vector ED methods and introduced a smear reduction technique. From the experimental results, it was found that both modified methods can improve color reproduction compared with the conventional method. The LAB method showed the best color reproduction performance ($\Delta E_{LAB} = 4.4$) and has spatial quality as good as the conventional method.

We believe that further improvement in color reproduction is possible by taking the actual printing property including dot gain into account.

Acknowledgment

The authors wish to thank Dr. M. A. Kriss of the University of Rochester for the useful discussion and the kind cooperation in preparing the manuscript. They also wish to thank the referees of this paper for their useful suggestions.

References

1. R. W. Floyd and L. Steinberg, "An adaptive algorithm for spatial greyscale," *Proc. SID* **17**, 75–77 (1976).
2. J. E Jarvis, C. N. Judice, and W. H. Ninke, "A survey of techniques for the display of continuous tone pictures on bilevel displays," *Computer Graphics and Image Processing* **5**, 13–40 (1976).
3. R. Ulichney, *Digital Halftoning*, MIT Press, Cambridge, MA (1987).
4. H. Kotera, "*Digital Halftoning*," *J. Inst. of Television Eng. of Japan* **40**(4), 317–323 (1986) (in Japanese).
5. T. N. Pappas, "Model-based halftoning of color images," *IS&T's 8th Intl. Congress on Advances in Non-impact Printing Technologies*, pp. 270–275 (1992).
6. Y. S. Kim and S. K. Kim, "Adaptive color error diffusion for natural color printing in binary color printer," *IS&Ts 9th Intl. Congress on Advances in Non-impact Printing Technologies*, pp. 583–586 (1993).
7. A H. Mutz and D. T. Lee, "An international standard for color facsimile," *IS&T and SID's 2nd Color Imaging Conf.*, pp. 52–54 (1994).

8. H. Ikegami *et al*, "Evaluation of color space for image communication focusing on color facsimile," *J. Inst. of Image EIectro. Eng. of Japan* **24**(1), 87–97 (1995) (in Japanese).
9. T. Kawamura, H. Haneishi, and Y. Miyake, "Color transformation between different imaging devices and its evaluation," *Display and Imaging* (in press).
10. P. C. Hung, "Colorimetric calibration in electronic imaging devices using a look-up-table model and interpolations," *J. Electronic Imaging* **2**(1), 53–61 (1993).
11. H. Haneishi, H. Yaguchi, and Y. Miyake, "A new method of color reproduction in digital halftone image," *IS&T's 46th Annual Conference Proc*., pp. 123–125 (1992).
12. H. Haneishi, N. Shimoyama and Y. Miyake, "Color digital halftoning color colorimetric color reproduction," *IS&T's Tenth Intl. Congress on Advances in Non-Impact Printing Technologies*, pp. 380–385 (1994).
13. C. Kim, S. Kim, Y. See, and I. Kweono, "Model-based color halftoning techniques on perceptually uniform color spaces," *IS&T's Annual Conference*, pp. 494–499 (1994).
14. H. E. J. Neugebauer, "Die theoretischen grundlagen des mehrfarbenbuchdrucks," *Z. Wiss Photo*. **36**(4), 73–89 (1937).
15. K. Kanamori and H. Kotera, "Analysis of color gamut for hardcopy based on Neugebauer theory," *Proc. SPIE* **1184**, 36–42 (1989).
16. R. W. G. Hunt, Reproduction of Color in Photography, Printing, and Television, Fountain Press, London (1987).

❋ Previously published in the *Journal of Electronic Imaging*, **5**(1) pp. 97–106, 1996.